



ARTICLE OPEN

The IFN- γ -p38, ERK kinase axis exacerbates neutrophilic chronic rhinosinusitis by inducing the epithelial-to-mesenchymal transition

Mingyu Lee^{1,2,3}, Dae Woo Kim⁴, Roza Khalmuratova¹, Seung-Hyun Shin^{2,3}, Yong-Min Kim⁵, Doo Hee Han⁶, Hyun-Jik Kim⁶, Dong-Young Kim⁶, Chae-Seo Rhee⁷, Jong-Wan Park^{1,2,3,8} and Hyun-Woo Shin^{1,2,3,6,8}

Chronic rhinosinusitis (CRS) is a heterogeneous and multifactorial inflammatory disease characterized by involvement of diverse types of inflammatory cells. Asian CRS patients frequently show infiltration of neutrophils and an elevated level of interferon (IFN)- γ ; by contrast, western patients exhibit eosinophil infiltration and enhanced levels of Th2-related cytokines. Neutrophilia in tissues decreases sensitivity to corticosteroids, but the mechanisms underlying the progression of neutrophilic CRS are unclear. In this study, we investigated the role of IFN- γ in CRS patients with marked neutrophil infiltration. We report that the IFN- γ level is upregulated in the tissues of these patients, particularly those with non-eosinophilic nasal polyps. The level of IFN- γ was significantly correlated with markers of the epithelial-to-mesenchymal transition (EMT). We further demonstrated that IFN- γ induced the EMT via the p38 and extracellular signal-regulated kinase (ERK) pathways in a manner distinct from the hypoxia-inducible factor (HIF)-1 α , SMAD, and NF- κ B signaling pathways. In a murine nasal polyp (NP) model, blocking the p38 and ERK signaling pathways prevented NP formation and chemotactic cytokine secretion by neutrophils but not eosinophils. Taken together, our results suggest that IFN- γ can induce the EMT in nasal epithelial cells, and thus blocking the p38 and ERK pathways could be an effective therapeutic strategy against neutrophil-dominant CRS.

Mucosal Immunology (2019) 12:601–611; <https://doi.org/10.1038/s41385-019-0149-1>

INTRODUCTION

Chronic rhinosinusitis (CRS) is a heterogeneous and multifactorial inflammatory disease of the paranasal sinuses and nasal cavities that affects 5–15% of the global population.¹ Accompanying nasal polyps (NPs) are suggestive of a recalcitrant and recurrent clinical course.² Two NP phenotypes are known; these differ in terms of the presence of eosinophilia: eosinophilic CRSwNP (E-NP) and non-eosinophilic CRSwNP (NE-NP).³ NPs are characterized as a Th2-dominant immunologic disease with pronounced eosinophilia and excessive expression of type 2 cytokines in western countries.⁴ However, the differences between Western and Asian patients with CRS suggest that CRS endotypes differ according to patient ethnicity.^{5,6} A recent report suggested that second-generation Asian patients with CRSwNP residing in the United States showed reduced eosinophilia, possibly resulting from their genetic background.⁷ Emerging evidence demonstrates that CRSwNP patients from Asian countries including Korea, Japan, Malaysia, and China show neutrophilic-type inflammation with the involvement of other T-cell subsets, such as Th1 and Th17 cells.^{5,8,9} Importantly,

a larger proportion of patients with NE-NP show neutrophil infiltration compared to those with E-NP.¹⁰ Furthermore, Tomassen et al. found high expression of IFN- γ even in patients that showed high positivity for interleukin (IL)-5.¹¹

Corticosteroids (CSs) are used to decrease the size of NPs and improve the nasal symptoms of E-NP patients.¹² Although increased neutrophilia in NPs reduces the response to oral corticosteroid therapy,¹³ little is known about the effect of neutrophil infiltration on the pathogenesis and treatment of NPs. Similarly, patients with severe asthma (SA) are characterized by neutrophil infiltration and are rarely responsive to systemic CSs.¹⁴ Given that neutrophils are producers of interferon (IFN)- γ , controlling IFN- γ signaling in NE-NP patients could be a powerful therapeutic strategy.

Recently, the epithelial-to-mesenchymal transition (EMT) has been observed in CRS and NP tissues, and is thought to be one of the pathophysiological processes in CRS.^{15,16} The EMT is a cellular process whereby epithelial cells acquire mesenchymal properties and lose cell-to-cell interactions and apicobasal polarity.¹⁷ Liu et al. showed that an inflammatory cytokine including IL-1 β , tumor

¹Obstructive Upper airway Research (OUAR) Laboratory, Department of Pharmacology, Seoul National University College of Medicine, Seoul, Korea; ²Department of Biomedical Sciences, Seoul National University Graduate School, Seoul, Korea; ³Cancer Research Institute, Seoul National University College of Medicine, Seoul, Korea; ⁴Department of Otorhinolaryngology-Head and Neck Surgery, Boramae Medical Center, Seoul, Korea; ⁵Department of Otorhinolaryngology-Head and Neck Surgery, Chungnam National University Hospital, Daejeon, Korea; ⁶Department of Otorhinolaryngology-Head and Neck Surgery, Seoul National University Hospital, Seoul, Korea; ⁷Department of Otorhinolaryngology-Head and Neck Surgery, Seoul National University Bundang Hospital, Seongnam, Korea and ⁸Ischemic/Hypoxic Disease Institute, Seoul National University College of Medicine, Seoul, Korea

Correspondence: Hyun-Woo Shin (charlie@snu.ac.kr)

Clinical Mucosal Immunology Study Group: Dae Woo Kim, Yong-Min Kim, Hyun-Woo Shin.

Received: 30 January 2018 Revised: 25 January 2019 Accepted: 4 February 2019

Published online: 25 February 2019



necrosis factor (TNF)- α , and IFN- γ enhanced the transforming growth factor (TGF)- β -induced EMT in A549 cells.¹⁸ In addition, Soyka et al. demonstrated that IFN- γ and/or IL-4 disrupted the epithelial barrier in an air-liquid interface (ALI) culture system.¹⁹ This increased epithelial permeability induced by IFN- γ was also reported in T84 colonic epithelial cells.²⁰ Moreover, an IFN consensus sequence-binding protein, the production of which was induced by IFN- γ treatment, was found to promote invasion and EMT-like phenomena in the osteosarcoma cell lines U2OS and Saos-2.²¹

In the present study, the effect of IFN- γ on the EMT was evaluated in patients with neutrophil-dominant CRS. Some of the results of this study were previously reported in abstract form.²²

RESULTS

Increased level of IFN- γ in patients with NE-NP

A multiplex enzyme-linked immunosorbent assay (ELISA) was performed to determine whether the IFN- γ level increases during the development of CRS. The IFN- γ concentrations in nasal-tissue extracts from 11 patients with CRSsNP, 82 patients with CRSwNP, and 6 control individuals were elevated according to CRS progression, with the highest level detected in the NP tissues (Fig. 1a). When the levels of IFN- γ were compared between patients with NE-NP and E-NP, as reported previously,²³ the NE-NP patients showed higher levels of IFN- γ (Fig. 1a). Because the number of neutrophils in tissues from NE-NP patients was significantly higher than in tissue from E-NP patients,¹⁰ we examined whether the majority of IFN- γ was produced by

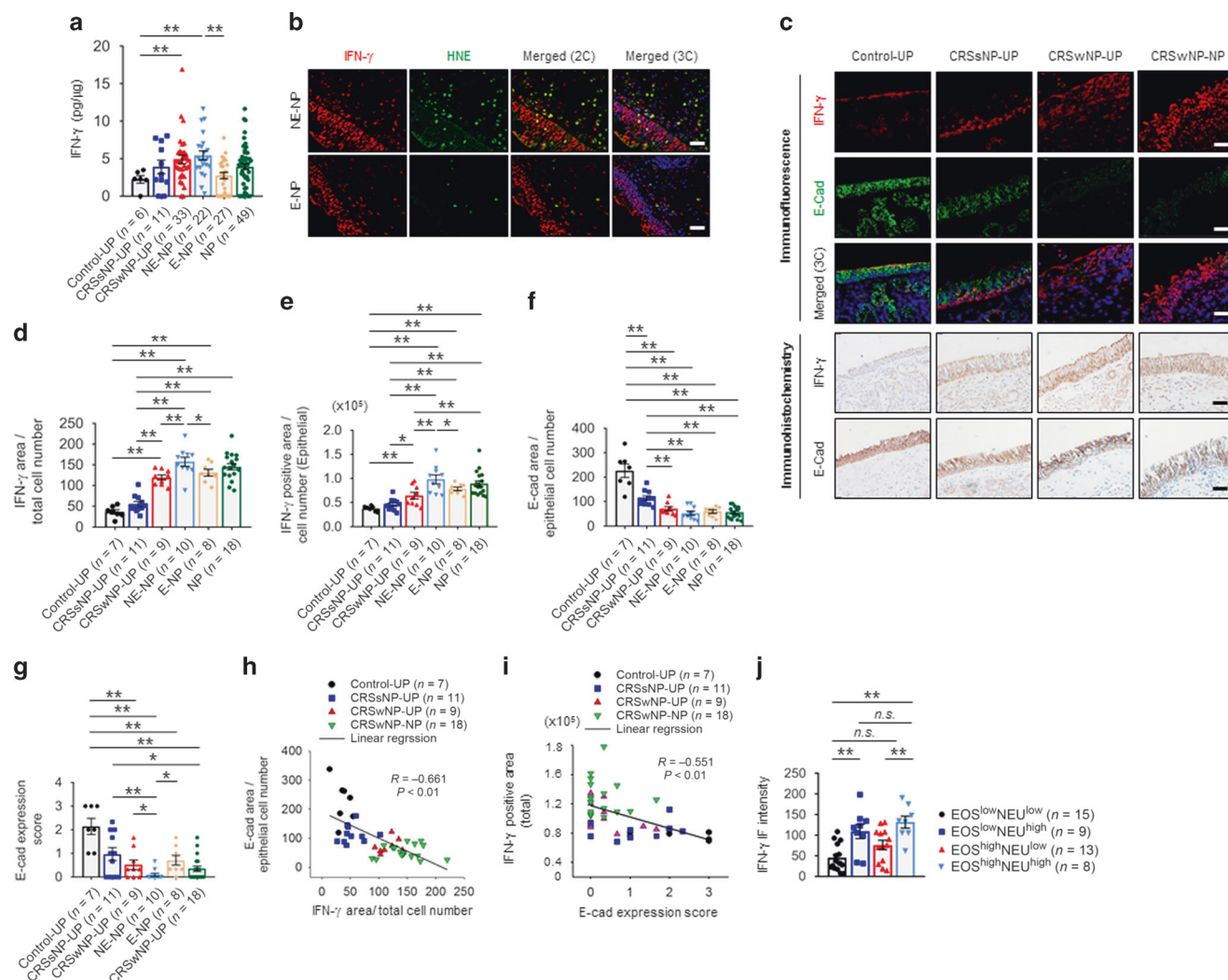


Fig. 1 Upregulation of interferon (IFN)- γ and reciprocal expression with E-Cad in patients with neutrophilic non-eosinophilic (NE) chronic rhinosinusitis with nasal polyps (CRSwNP). **a** The concentration of IFN- γ was measured by ELISA and compared ($n = 6, 11, 33, 22, 27, 49$ from left to right). **b** Co-immunofluorescence staining of IFN- γ (red) and neutrophil elastase (green) in tissues from patients with NE-NP and E-NP. Representative immunofluorescence images were acquired. **c** Double immunofluorescence (IF) staining and immunohistochemistry (IHC) in uncinata process (UP) mucosa from control patients without nasal disease ($n = 7$), UPs from patients with CRSsNP ($n = 11$), and UP ($n = 9$) and NP ($n = 18$) tissues from patients with CRSwNP. IFN- γ (red) and E-Cad (green) was stained for immunofluorescence and brown (for IHC). Representative images were acquired. **d-f** Immunofluorescence and immunohistochemical intensities of IFN- γ and E-Cad were quantified by ImageJ software in the patient groups as indicated above. **g** E-Cad expressions were examined in a high power field (HPF; $\times 400$) and scored from 0 to +3. Detailed information for scoring the E-Cad expression is provided in supplementary information. **h** Correlation of IFN- γ and E-Cad immunofluorescence intensities in each of patient groups. **i** Correlation of IFN- γ immunohistochemical intensity and E-Cad expression score. **j** Immunofluorescence intensity of IFN- γ following the proportion of EOS/NEU in indicated patients. Statistical significance (**a, d-g, j**) was determined by Kruskal-Wallis tests ($P < 0.01$), followed by Mann-Whitney U -test for pairwise comparisons. Spearman correlation test (**h, i**) was used. Spearman r values and the corresponding P -values were calculated. * $P < 0.05$; ** $P < 0.01$; n.s. not significant. Data are shown as means \pm s.e.m. Scale bar, 50 μ m (**b, c**)

neutrophils. We evaluated the level of IFN- γ and the number of neutrophils in tissue from patients with NE-NP and E-NP by co-immunofluorescence (IF) staining. IFN- γ -positive cells (red) were observed in the epithelium and sub-epithelium areas (Fig. 1b). Above all, we found that IFN- γ /neutrophil elastase (NE) double-positive cells (neutrophils) were the most abundant cell types among the IFN- γ positive immune cells (Fig. 1b). The numbers of double-positive cells for IFN- γ and immune cells, such as eosinophils, neutrophils, T cells, NK cells, and B cells in tissues from both E-NP patients and NE-NP patients were presented in Figure S1A,B. Interestingly, epithelial cells also showed high-level expression of IFN- γ , suggesting that they contribute to IFN- γ -related responses (Fig. 1b, c). No significant signal was detected after staining of serial sections of tissues from NP patients with rabbit or mouse IgG (negative control). Our data revealed that the expression of IFN- γ in neutrophils and epithelial cells was increased in NE-NP patients (Fig. 1b).

Reciprocal expression of IFN- γ and E-cad in tissues in patients with CRS

We previously reported that expression of E-cad is frequently lost in NP epithelial cells and that this is characteristic of the EMT.²⁴ Therefore, we investigated the relationship between IFN- γ and E-cad by IF and immunohistochemistry (IHC). We observed weak IFN- γ positivity in uncinate processes (UPs) from control and CRSsNP subjects, together with intense E-cad staining in the mucosal epithelium. However, IFN- γ expression was slightly elevated in UP tissues and was notably increased in the tissues from CRSwNP patients. In contrast, E-cad expression was reduced in those patients (Fig. 1c–g). Consistent with the ELISA results (Fig. 1a), IFN- γ expression was higher in patients with NE-NP (Fig. 1d, e and S2A, B). The intensity of the IFN- γ signal was negatively correlated with that of E-cad (Fig. 1h; Spearman's correlation coefficient, $P < 0.01$). Similarly, the IFN- γ IHC signal intensity was negatively correlated with the E-cad expression score (Fig. 1i; Spearman's correlation coefficient, $P < 0.01$). When patients were categorized into four groups according to their eosinophil and neutrophil counts, IFN- γ expression was upregulated in the eosinophil^{low}/neutrophil^{high} NP groups compared with the eosinophil^{low}/neutrophil^{low} NP groups (Fig. 1j). Taken together, these findings suggest that IFN- γ contributes to the loss of E-cad.

IFN- γ promotes the EMT in human nasal epithelial cells

Next, we tested whether the EMT could be induced in nasal epithelial cells by IFN- γ . We also examined the following other inflammatory mediators: representative cytokines that are upregulated in Th1, Th2, and Th17 inflammation (TNF- α , IFN- γ , IL-5, and IL-17A), a major cytokine produced by epithelial cells (IL-6), and neutrophil and eosinophil chemotactic cytokines (IL-8, CCL11, and CCL24). Among these factors, IFN- γ potentially decreased the expression of epithelial markers (E-cad and β -CTN). However, it increased the levels of mesenchymal markers (α -SMA and Vimentin) and known EMT-inducing factors (Snail and Twist) (Fig. 2a). Densitometry analysis of protein levels normalized to that of β -tubulin is shown in Fig. 2b. In phalloidin-stained hNECs, IFN- γ treatment induced the formation of lamellipodia (Fig. 2c). As reported previously, IFN- γ induced the upregulation of HIF-1 α even under normoxic conditions, which induced loss of E-cad.²⁴ Considering that SIRT1 suppressed the HIF-1 α -induced EMT,¹⁶ the effect of IFN- γ on SIRT1 and HIF-1 α expression was evaluated. We found that IFN- γ treatment resulted in upregulation of HIF-1 α and downregulation of SIRT1 levels (Figure S3A, B). We next evaluated IFN- γ -mediated induction of the EMT at an ALI, which more closely mimics the in vivo conditions and enables evaluation of airway epithelial function.^{25,26} We first assessed the differentiation status of epithelial cells maintained under ALI conditions for 21 days. Incubation under ALI conditions induced the formation of a

pseudostratified and differentiated epithelium that contained goblet cells (stained with Mucin 5AC), ciliated cells (stained with ac-tubulin), and tightly joined epithelial cells (stained with E-cad) (Fig. 2d). Although the connections among fully differentiated epithelial cells were stronger than those among epithelial cells in submerged condition, IFN- γ treatment could change the EMT markers (Fig. 2e). Densitometry analysis of protein levels normalized to that of β -tubulin is shown in Fig. 2f. The morphology of hNECs cultured under submerged or ALI conditions changed from a cobblestone-like phenotype to a fibroblast-like shape after IFN- γ treatment (Fig. 2g). However, the other cytokines did not induce changes towards an EMT-like phenotype in hNECs (Figure S3C). The relative changes in E-cad and α -SMA levels were validated by IF staining. IFN- γ -treated hNECs exhibited decreased E-cad expression and increased α -SMA expression (Fig. 2h and S3D). Thus, we conclude that IFN- γ is sufficient to induce the EMT in hNECs.

IFN- γ triggers the EMT via the p38 and ERK signaling pathways To evaluate the effect of IFN- γ on induction of the EMT, we investigated its related intracellular signaling pathways—the JAK-STAT1, NF- κ B, ERK1/2, and p38 pathways.^{27–29} Stimulation of hNECs with IFN- γ resulted in upregulation of the levels of p-JAK1,2, p-STAT1, p-ERK1/2, and p-p38, but not that of p-p65 (ser276) or p-p65 (ser536) (Fig. 3a). IFN- γ had no effect on the luciferase activity of RPMI2650 cells transfected with NF- κ B luciferase plasmid DNA (Figure S4A). Furthermore, the nuclear level of NF- κ B was not influenced by IFN- γ treatment (Fig. 3b). Therefore, NF- κ B signaling may not be involved in IFN- γ -mediated induction of the EMT. To determine whether induction of the EMT by IFN- γ was mediated by STAT1, hNECs were transfected with a small interfering RNA (siRNA) targeting STAT1. STAT1 knockdown blocked the IFN- γ -mediated induction of the EMT in hNECs (Fig. 3c and S4B, 4D). IFN- γ stimulation reportedly induces the production of interferon consensus sequence-binding protein (ICSBP) through STAT1, and ICSBP activates TGF- β , p38, and ERK signaling.^{21,30} In this study, IFN- γ treatment resulted in upregulation of the mRNA and protein levels of ICSBP (Fig. 3d). Interestingly, ICSBP knockdown also inhibited the IFN- γ -mediated induction of the EMT (Fig. 3e and S4C, D). However, IFN- γ stimulation did not induce the activation of SMAD2 and SMAD3 (Fig. 3f). Moreover, silencing of SMAD3 did not influence the IFN- γ -mediated induction of the EMT (Figure S5A–C). Because HIF-1 α induces the EMT in nasal epithelial cells,²⁴ and this effect is enhanced by IFN- γ (Figure S3A), we also examined the effect of HIF-1 α silencing on IFN- γ -mediated induction of the EMT. Similar to the SMAD3 silencing results, the HIF-1 α pathway exerted a minor effect on IFN- γ -mediated induction of the EMT in hNECs (Figure S5D–F). Therefore, we investigated the relationship between ICSBP and p38 and ERK signaling. ICSBP knockdown reduced the expression of p-p38 and p-ERK, whereas inhibition of p38 and ERK signaling did not affect STAT1 phosphorylation or ICSBP expression (Fig. 3g, h). Taken together, these data suggested that the IFN- γ -mediated induction of the EMT in hNECs is dependent on JAK-STAT1-ICSBP-p38 and ERK signaling. We next determined by IHC the expression levels of p-p38 and p-ERK in tissues from CRS and NP patients; the expression levels of p-ERK and p-p38 increased with CRS progression. Importantly, the NE-NP patients showed the highest p-p38 and p-ERK expression levels (Fig. 3i–k). Moreover, the eosinophil^{low}/neutrophil^{high} NP groups exhibited high p-p38 and p-ERK expression levels (Figure S6A, B). Therefore, p38 and ERK may be therapeutic targets for preventing IFN- γ -mediated induction of the EMT.^{28–30}

p38 and/or ERK inhibitors recapitulate the EMT phenotype in polyp-derived epithelial cells

To clarify the effect of MAPK signaling on the IFN- γ -mediated induction of the EMT, we used a p38 inhibitor (SB203580) as well

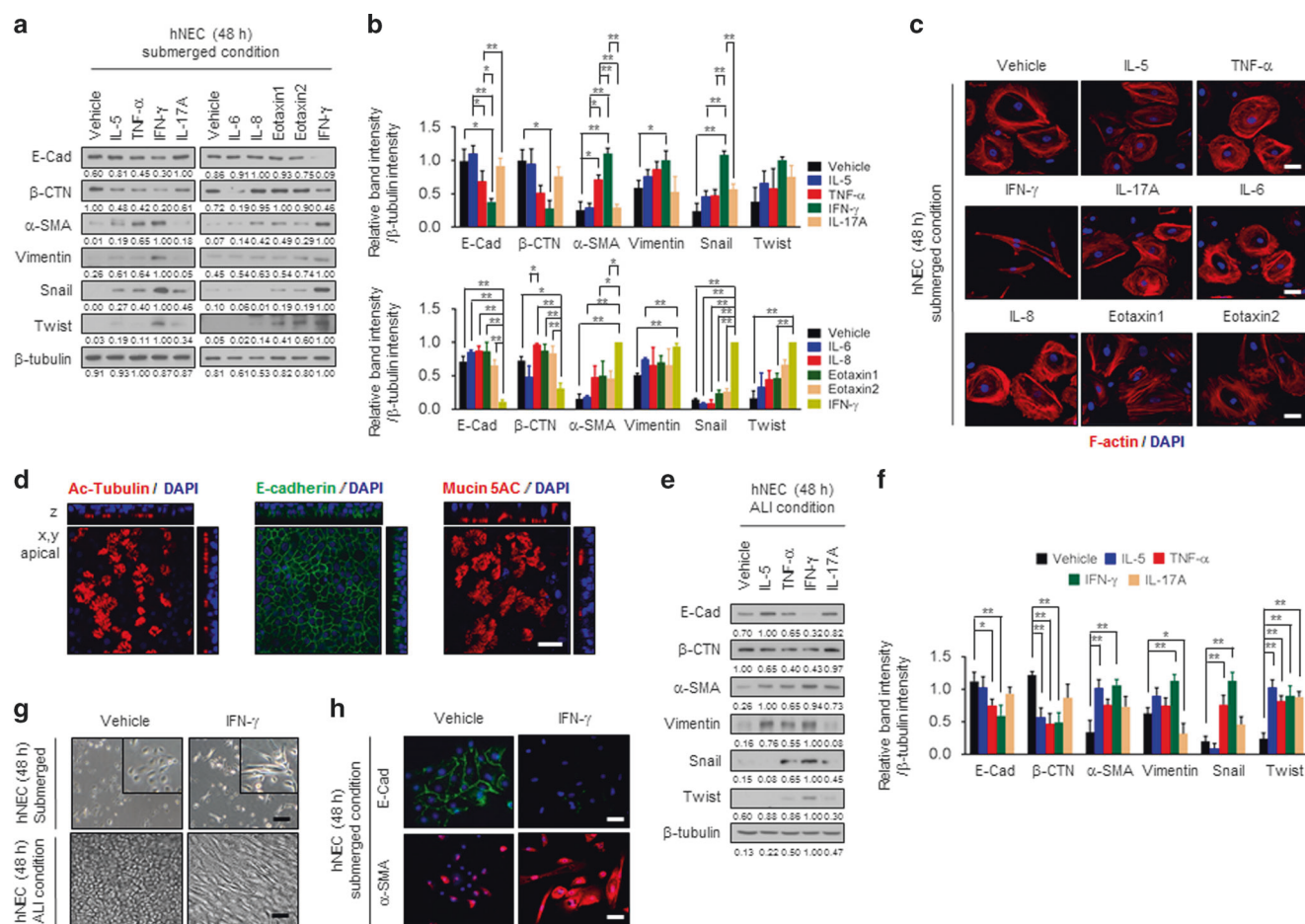


Fig. 2 IFN- γ induced epithelial-to-mesenchymal transition (EMT) in human nasal epithelial cells (hNECs). **a** hNECs in submerged conditions were cultured with each type of cytokines (100 ng/ml) and incubated for 48 h. EMT markers were traced. **b** Each data are expressed as normalized band intensity adjusted to β -tubulin, which serves as loading control. **c** Representative images of hNECs treated with indicative cytokines (100 ng/ml) for 48 h were stained with phalloidin, which labels F-actin. **d** Representative z-stack confocal photographs of differentiation markers were acquired. ALI-cultured cells were incubated with anti-ac-tubulin (for ciliated cells), anti-Mucin 5AC (for goblet cells) and anti-E-Cad antibodies, respectively. **e** hNECs in ALI conditions were cultured with indicated cytokines (100 ng/ml) and incubated for 48 h. EMT markers were traced. **f** Each data are expressed as normalized band intensity adjusted to β -tubulin, which serves as loading control. **g** Representative phase contrast images of hNECs were acquired after treatment of IFN- γ (100 ng/ml) in submerged or ALI conditions. **h** hNECs were treated with or without IFN- γ (100 ng/ml) for 48 h in submerged conditions. Cells were immunostained against EMT markers (E-Cad, α -SMA) and visualized. In all immunoblot analysis, protein intensities (**a**, **e**, **f**) were quantified by ImageJ software ($n = 1$, three independent experiments). Representative western blots (**a**, **e**) are depicted and expressed as relative band intensity adjusted to the highest band intensity of each protein. Statistical significance (**b**, **f**) for normalized band intensity was determined by Student's t -test. * $P < 0.05$; ** $P < 0.01$. Data are shown as means \pm s.e.m. Scale bars, 50 μ m (**c**, **d**, **g**, **h**)

as a MEK inhibitor (PD98059). The IFN- γ -induced spindle-shaped morphology of hNECs was restored by SB203580 and/or PD98059 treatment (Fig. 4a). Similarly, the inhibitors reversed the IFN- γ -induced suppression of the levels of epithelial markers (E-cad and β -CTN), as well as induction of the mesenchymal markers (α -SMA, Vimentin, Twist, and Snail) (Fig. 4b). In particular, co-inhibition of p38 and ERK resulted in more prominent reversal of the changes in the levels of EMT markers than did inhibition of either alone. We next determined whether application of a mixture of p38 and ERK inhibitors could reverse the mesenchymal phenotype in polyp-derived epithelial cells using polyps from neutrophilic CRSwNP patients. We first investigated the characteristics of primary human nasal epithelial cells cultured under ALI conditions (seven cells from controls and seven cells from NE-NP patients) by immunoblotting. Polyp-derived epithelial cells showed a mesenchymal phenotype, as indicated by their expression of EMT markers, as mentioned above. Densitometry analysis of protein levels normalized to that of β -tubulin is shown in Fig. 4c. Finally, we treated fully differentiated ALI-cultured epithelial cells

with the inhibitor mixture; this treatment reversed the changes in the levels of most of the EMT markers. Densitometry analysis of protein levels normalized to that of β -tubulin is shown in Fig. 4d. These observations imply that p38 and ERK are essential for IFN- γ -mediated induction of the EMT.

Inhibition of p38 and ERK suppresses IFN- γ -induced migration
We next evaluated the influence of p38 and ERK inhibition on the migratory capacity of hNECs. As expected, IFN- γ treatment significantly increased the migration of hNECs. However, blocking of p38 and ERK signaling reduced the number of migrating cells (Fig. 5a, b). Consistent with this finding, IFN- γ -treated hNECs had many long F-actin stress fibers (signifying an increased migration capacity), the number of which was substantially reduced by inhibition of p38 and ERK signaling (Fig. 5c). A methyl thiazolyl tetrazolium (MTT) assay showed that there was no significant difference in cytotoxicity between the three groups (Fig. 5d). We next evaluated the migratory capacity of IFN- γ -treated hNECs with an in vitro wound-healing assay. We observed that IFN- γ -treated

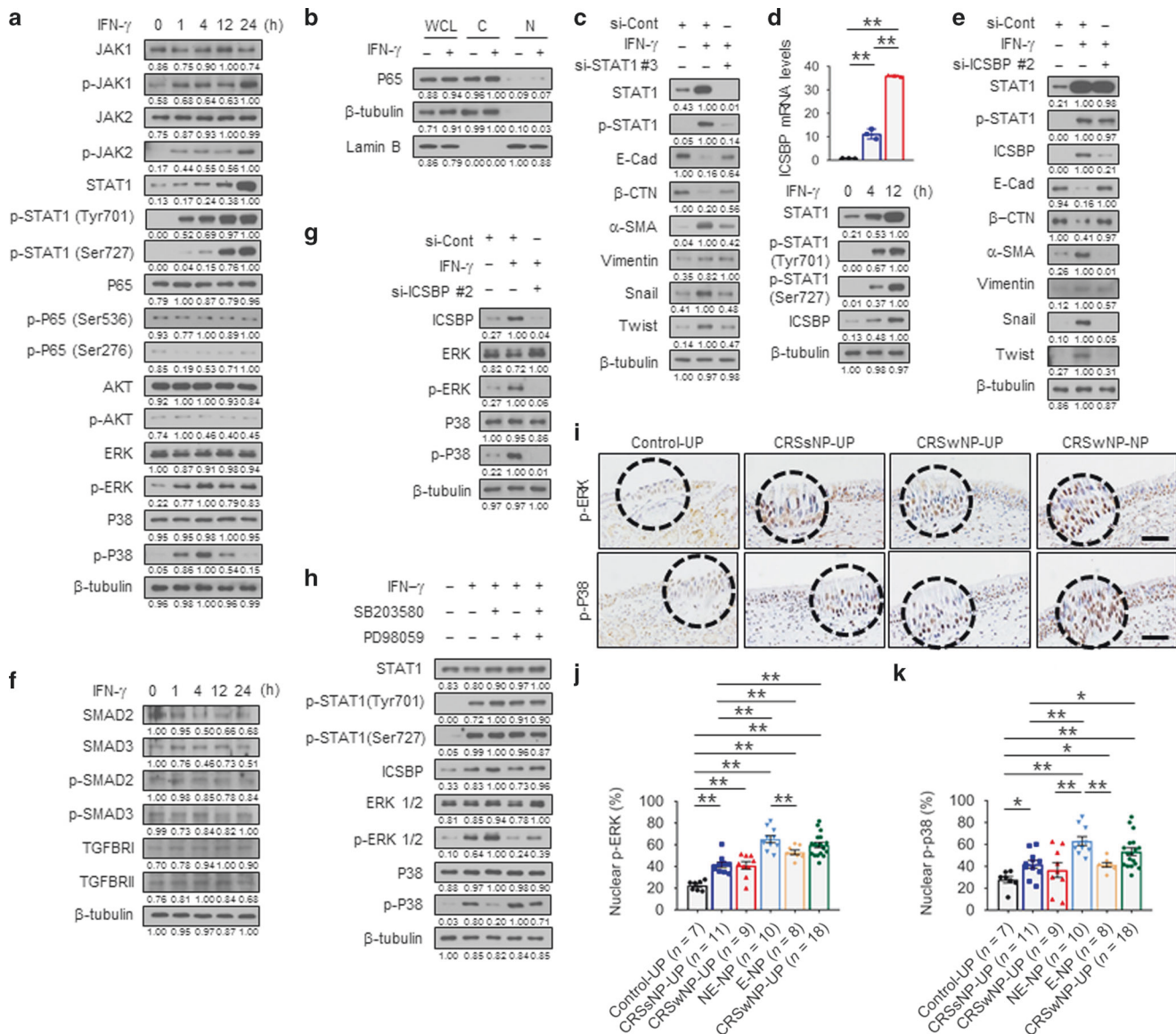


Fig. 3 p38, ERK signaling is crucial for IFN- γ -induced EMT in hNECs and is activated in patients with neutrophilic NE-NP. **a** hNECs treated with IFN- γ (100 ng/ml) in a time-dependent manner were immunoblotted using the indicated antibodies. **b** Western blot analyses of cytoplasmic (C) and nuclear (N) fractions from confluent hNECs, which had been treated with or without IFN- γ . **c** STAT1-knockdown hNECs were treated with IFN- γ for 48 h. Immunoblots were performed on cell lysates with indicated antibodies. **d** Real-time qRT-PCR and western blot to analyze expression of ICSBP for the indicated times after treatment of IFN- γ . **e** ICSBP-knockdown hNECs were treated with IFN- γ for 48 h. Cell lysates were immunoblotted with the indicated antibodies. **f** Immunoblot analysis in hNECs treated with IFN- γ for the indicated times. **g** ICSBP-knockdown hNECs were cultured with IFN- γ for 48 h. Activation of p38, ERK was evaluated by using western blot. **h** hNECs were pre-treated with p38 inhibitor (SB203580), ERK inhibitor (PD98059) respectively or both followed by IFN- γ stimulation for 8 h. Cell lysates were immunoblotted with indicated antibodies. **i** Immunohistochemical staining of phospho-p38 and phospho-ERK in UP mucosa from control patients without nasal disease ($n = 7$), UPs from patients with CRSwNP ($n = 11$), and UP ($n = 9$) and NP tissues ($n = 18$) from patients with CRSwNP. Scale bars, 50 μ m. **j** Comparison of nuclear p38, ERK expression in the same patients as indicated above. In all immunoblot analysis (**a**–**h**), protein intensities were quantified by ImageJ software ($n = 1$, three independent experiments). Representative western blots are depicted and expressed as relative band intensity adjusted to the highest band intensity of each protein. The data are representative of three independent experiments with similar results. Statistical significance was determined by Student's *t*-test (**d**) and Kruskal–Wallis tests ($P < 0.01$), followed by Mann–Whitney *U*-test for pairwise comparisons (**j**, **k**). * $P < 0.05$; ** $P < 0.01$. Data are shown as means \pm s.e.m

hNECs showed a ~20% increase in migration compared with vehicle-treated control cells (Figure S7A, B), which resulted in accelerated wound closure. Additionally, we evaluated the impact of IFN- γ on the barrier function of differentiated hNECs by monitoring transepithelial resistance (TEER) in the presence and absence of IFN- γ . IFN- γ significantly reduced the mean TEER in a time-dependent manner compared with the vehicle-treated controls. In contrast, p38 and ERK inhibition restored some, but not all, of the epithelial integrity (Fig. 5e). These results revealed

that IFN- γ enhances the migratory capacity of hNECs and epithelial dysfunction.

Effects of p38 and ERK inhibitors on polyp formation in a murine polyp model

We next investigated the effects of p38 and ERK inhibitors on polyp formation using a previously established murine NP model (Fig. 6a).³¹ Polyp-bearing mice exhibited prominent NPs, epithelial disruptions, and higher IFN- γ expression compared to

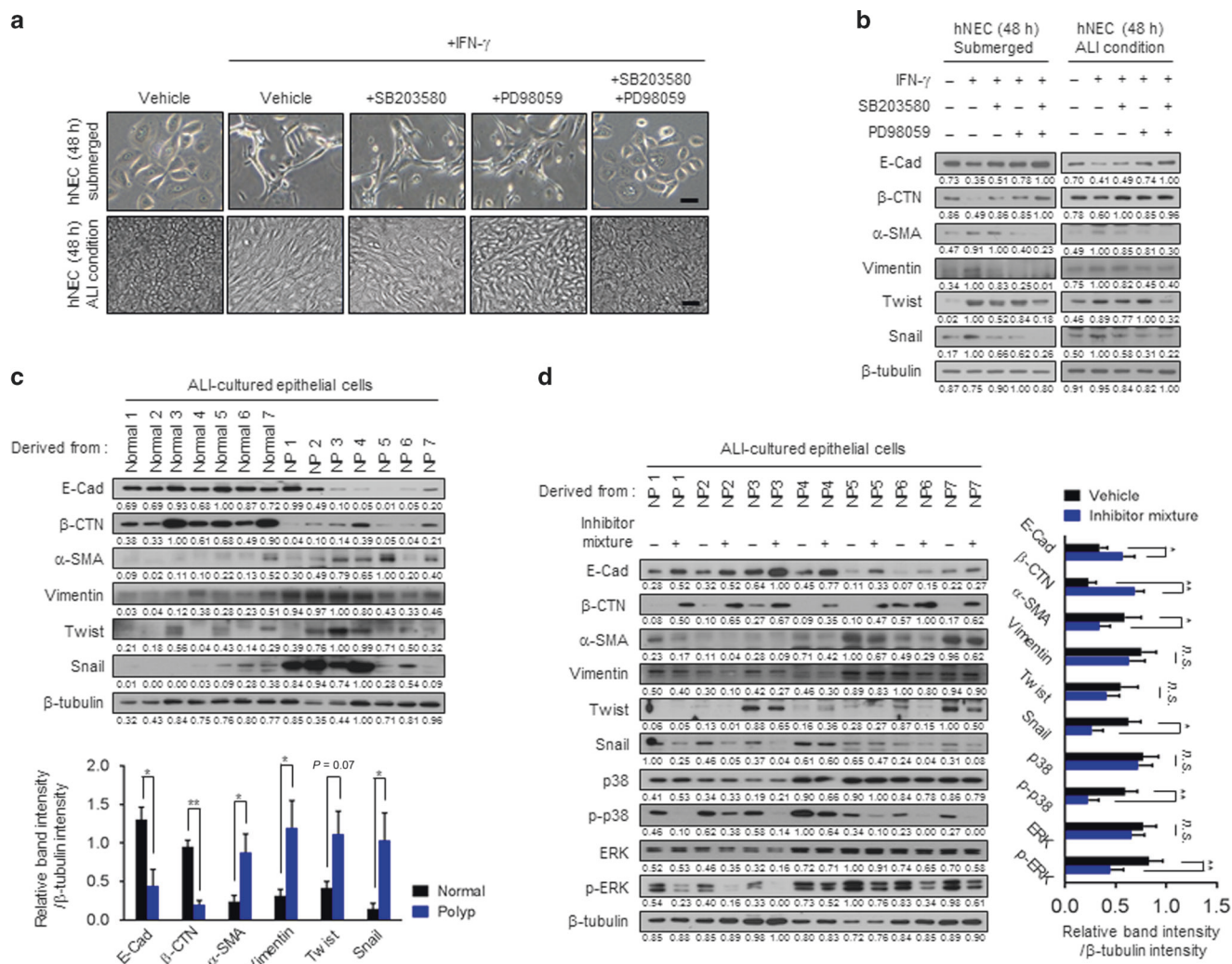


Fig. 4 Inhibition of p38, ERK signaling restores EMT. **a** Fully differentiated or submerged hNECs were pre-treated with p38 inhibitor (SB203580), ERK inhibitor (PD98059) respectively or both followed by incubation with IFN- γ for 48 h. Representative phase-contrast images of cells were acquired and cell lysates were immunoblotted with indicated antibodies (**b**). Scale bars, 50 μ m. **c** Comparison of epithelial characteristics derived from normal and patient with CRSwNP. Each of the ALI cultured primary nasal epithelial cells were lysed and evaluated by immunoblot. Densitometric quantification of three separate blots. **d** Fully differentiated nasal epithelial cells derived from CRSwNP patients were treated with the mixture of p38, ERK inhibitors for 48 h. Indicated proteins were assessed by immunoblot. Densitometric quantification of three separate blots. In all immunoblot analysis, protein intensities (**b–d**) were quantified by ImageJ software ($n = 1$, three independent experiments). Representative western blots (**b–d**) are depicted and expressed as relative band intensity adjusted to the highest band intensity of each protein. Each data (**c, d**) are expressed as normalized band intensity adjusted to β -tubulin, which serves as loading control. The data are representative of three independent experiments with similar results. Statistical significance for normalized band intensity was determined by Student's t -test (**c**) and Wilcoxon signed-rank test (**d**). * $P < 0.05$; ** $P < 0.01$; n.s. not significant. Data are shown as means \pm s.e.m

phosphate-buffered saline (PBS)-treated control mice (Fig. 6b–f and S8A, B). The criteria used to classify NPs and epithelial disruptions are provided in Figure S9A–C. Administration of ovalbumin (OVA) and *Staphylococcus aureus* enterotoxin B (SEB) resulted in upregulation of the IFN- γ mRNA and protein levels in NP tissue (Fig. 6e, f). As the mice with NPs showed a mixed pattern of inflammation (including Th1, Th2, and Th17 types³¹), we counted the number of infiltrating neutrophils by IHC. OVA/SEB-treated mice exhibited approximately 15 neutrophils per high-power field (Fig. 6g, h); this number, as well as the number of NP lesions, was decreased by application of the p38 and ERK inhibitors (Fig. 6c, d). Consistently, IFN- γ neutralization also reduced the IFN- γ expression, the number of nasal polyps and the number of epithelial disruptions (Figure S10A–E). Importantly, blocking p38 and ERK signaling led to downregulation of IFN- γ expression, number of neutrophils, and the levels of the

neutrophil chemotactic cytokines CXCL1 and CXCL2 (Fig. 6e–j and S8A, B). By contrast, dexamethasone suppressed the eosinophilic characteristics of the tissue samples, such as the levels of the eosinophil chemotactic cytokines CCL11 and CCL24. Furthermore, CDH1 expression was downregulated and that of ACTA2 upregulated in the OVA/SEB-treated mice; these changes were reversed by treatment with the inhibitor mixture and dexamethasone (Fig. 6k, l). Interestingly, administration of the inhibitor mixture did not affect the expression levels of proinflammatory cytokines such as IL4, IL13, and IL17A (Figure S11A–C) or those of the T-cell-subset-specific transcription factors TBX21 (Th1), GATA3 (Th2), and ROR γ (Th17) (Figure S11D–F). These findings suggest that the inhibitor mixture exerted anti-inflammatory and anti-polyp effects by inhibiting the establishment of neutrophilic features during the development of neutrophilic CRS. Because a large proportion of Asian CRS patients with or without

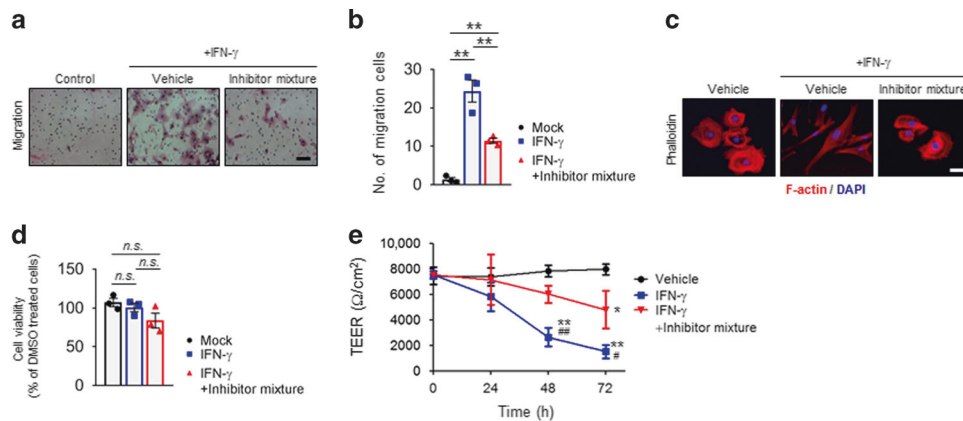


Fig. 5 IFN- γ promotes cell migration potential. **a, b** Representative images of hNECs migrating through Transwell inserts toward serum for 48 h. Cells were cultured with IFN- γ (100 ng/ml) alone or in combination with inhibitors. Cells that migrated to the lower surface of the filters were quantified. Photographs were taken at $\times 40$ magnification and are presented in the bar graph. Statistical significance was determined by Kruskal–Wallis tests ($P < 0.05$), followed by Mann–Whitney *U*-test for pairwise comparisons. ** $P < 0.01$. Data are shown as means \pm s.e.m ($n = 3$). **c** Representative F-actin (red) images of hNECs and MTT assay results (**d**) under resting conditions or stimulated with IFN- γ alone or in combination with p38, ERK inhibitors for 48 h. Scale bars, 50 μ m. Statistical significance was determined by Kruskal–Wallis tests ($P > 0.05$), followed by Mann–Whitney *U*-test for pairwise comparisons. n.s. not significant. Data are shown as means \pm s.e.m ($n = 5$). **e** The transition of TEER was measured after treatment of IFN- γ (100 ng/ml) alone or in combination with inhibitor mixtures. Resistance was measured at 24 h intervals from 0 to 72 h. Statistical significance was determined by Kruskal–Wallis tests ($P < 0.05$), followed by Mann–Whitney *U*-test for pairwise comparisons in each time point. Significant differences are denoted relative to vehicle (* $P < 0.05$, ** $P < 0.01$) or to the IFN- γ + inhibitor mixture treatment group (# $P < 0.05$, ## $P < 0.01$). Data are shown as means \pm s.e.m ($n = 3$)

NPs who exhibit reduced responsiveness to oral corticosteroid therapy also have neutrophilia, blocking p38 and ERK signaling could improve the clinical outcomes of these patients.

DISCUSSION

Tissue eosinophilia has generally been considered a main histologic characteristic of NPs and is reportedly present in 80–90% of all cases in western countries.^{3,4} Therefore, IL-5, a survival factor for eosinophils, was thought to play a crucial role in the pathogenesis of CRSwNP. However, a growing body of evidence suggests the existence of immunologic endotypes of CRS and NPs, and the Th1/Th2/Th17 cytokine profiles of CRSwNP patients vary geographically. Patients with CRSwNP from Europe and the United States exhibit Th2-biased eosinophilic inflammation, whereas a large proportion of Chinese patients in Beijing have a mixed pattern (Th1/Th2/Th17) of inflammation, and patients from Chengdu have still-lower expression of Th2 cytokines.^{5,6,8,10} Interestingly, some CRSwNP patients exhibit low IL-5 positivity together with neutrophilic inflammation.^{8,10} The fact that CRSsNP and CRSwNP patients with neutrophilic infiltration have an elevated level of IFN- γ suggests that IFN- γ plays a critical role in the development of neutrophilic CRS. However, the role of IFN- γ in the progression of CRS was unclear.

IFN- γ has significant roles not only in innate immunity against potential pathogens but also in adaptive immunity in orchestrating leukocyte attraction, maturation, and differentiation of many cell types.²⁸ This cytokine is a hallmark of the Th1 milieu that is abundant in many inflammatory diseases, including CRS.^{5,6} E-NP and NE-NP are the major subtypes of CRSwNP. However, whether the IFN- γ level is higher in patients with NE-NP compared to those with E-NP was unclear.^{9,32,33} Our findings revealed that the expression of IFN- γ was elevated in NE-NP patients (Fig. 1a), predominantly in those in the eosinophil^{low}/neutrophil^{high} group (Fig. 1j). The IFN- γ level in CRS patients in Asian countries is reportedly high,^{5,6} while that in CRS patients from western countries is low, suggesting that regional differences contribute to the differences among the CRS endotypes.

The EMT of epithelial cells is a prominent characteristic of upper and lower airway diseases, including CRS and asthma.¹⁵ Epithelial

cells from both CRSsNP and CRSwNP patients exhibit a mesenchymal phenotype and epithelial hyperplasia.^{34,35} However, the role of the EMT in the development of CRS is not fully understood. We reported previously that the hypoxic environment in CRSwNP could induce the EMT via HIF-1 α and p-SMAD3.²⁴ Here, we report that neutrophil-derived IFN- γ induced the EMT in hNECs via the JAK-STAT1-ICSBP-p38 and ERK signaling pathways. Importantly, p38 and ERK inhibitors suppressed NP formation and reversed the changes in the levels of EMT markers (Figs. 4–6). Thus, we speculate that the IFN- γ -induced EMT may be a therapeutic target in CRS and/or NP patients with marked neutrophilia.³⁵ However, the mechanism by which the EMT leads to polyp growth is unclear. It is possible that loss of plasma membrane proteins such as E-cad, ZO-1, and occludin during the EMT leads to excessive proliferation and remodeling of the sinonasal epithelium.^{36,37} Reversal of the EMT based on their mechanism could suppress nasal polypogenesis in several reports.^{3,8} In this perspective, the EMT may be involved in NP formation. To the best of our knowledge, this is the first study to report an association between a proinflammatory cytokine and the EMT in nasal polypogenesis.

SA patients exhibit neutrophilic infiltration and enhanced Th1 immune responses (including the IFN- γ level) in the airways.^{14,38} This complicates the treatment of patients with SA, as they are not responsive to high doses of systemic CSs.³⁹ Similarly, neutrophilia reduces the responsiveness of NE-NP patients to oral corticosteroid therapy.¹³ In this study, patients with NE-NP showed marked infiltration of neutrophils, most of which secreted IFN- γ (Fig. 1a, b). Because IFN- γ induced the EMT via the JAK-STAT1-ICSBP-p38 and ERK signaling pathways, suppression of p38 and ERK may be a more effective treatment for NE-NP than CS therapy.

Interestingly, the IFN- γ -induced EMT in airway epithelial cells was not influenced by HIF-1 α and TGF- β signaling (Fig. 3f and S5). Hypoxia is a critical stimulant of HIF-1 α activation, and we previously showed that HIF-1 α is the main factor that induces the EMT under hypoxic conditions in hNECs.²⁴ Although HIF-1 α expression was induced by IFN- γ treatment (Figure S3A, B), silencing of HIF-1 α did not reverse the EMT, as confirmed by the levels of EMT markers (Figure S5D–F). TGF- β , a proinflammatory cytokine, weakens epithelial integrity and promotes mesenchymal

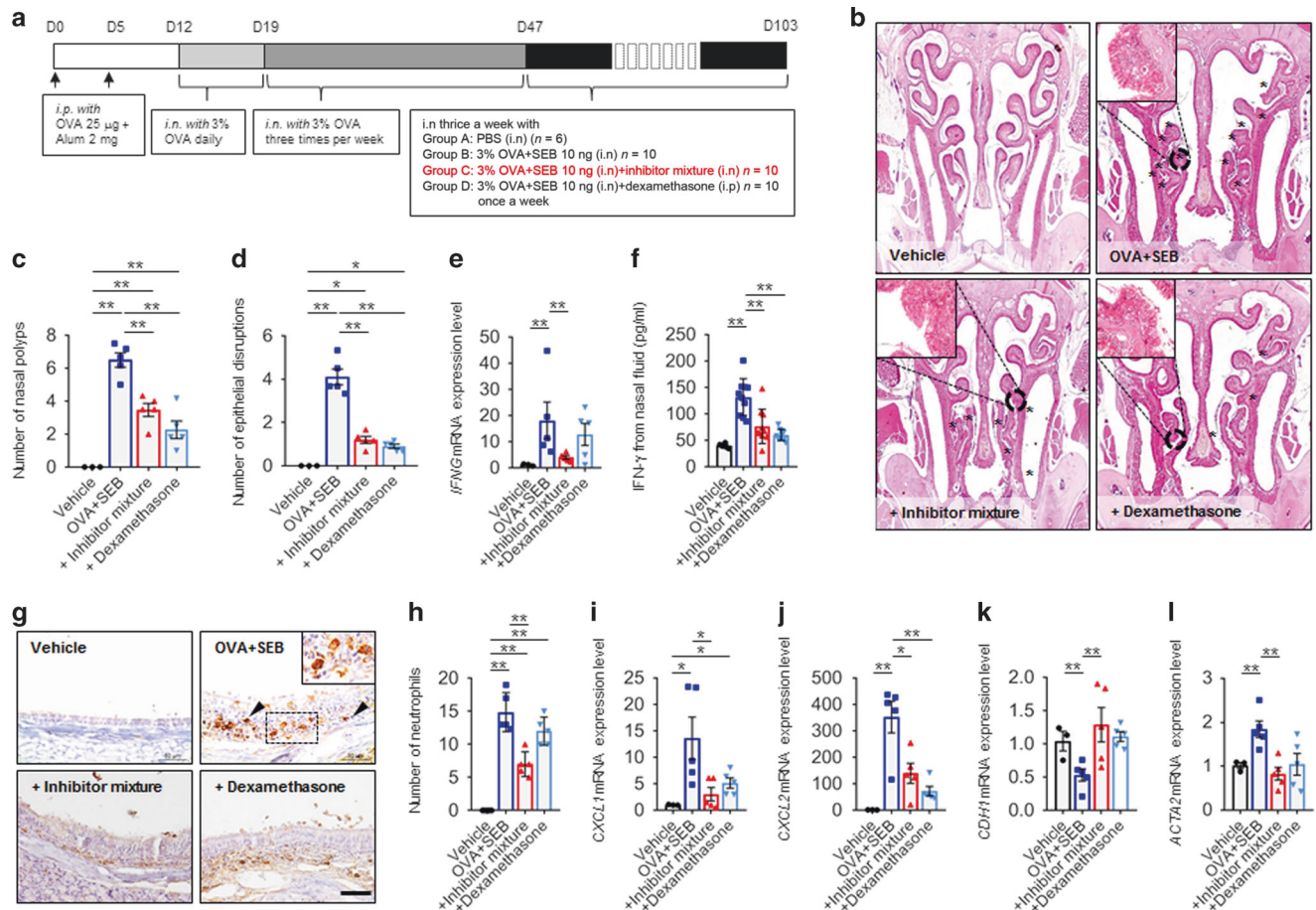


Fig. 6 Effect of ERK and p38 inhibitors on polyp formation in mice. **a** Schematic illustration of the murine NP model. BALB/c mice were treated with ovalbumin (OVA), *Staphylococcus enterotoxin B* (SEB), and a mixture of p38, ERK inhibitors; i.p. intraperitoneal, i.n. intranasal. **b** Representative photographs of sinonasal spaces and polypoid lesions stained with H&E in the indicated groups. Asterisk denotes the NP lesions in mouse nasal mucosa. Representative photographs were taken at $\times 40$ magnification. Areas indicated with squares are shown as magnified images. **c**, **d** Numbers of polypoid lesions and epithelial disruptions were counted and compared. **e** Relative *IFNG* mRNA expression in mucosal tissues from each group of mice was compared. **f** Protein levels of IFN- γ from nasal fluid were measured by ELISA and compared. **g** Representative images of immunohistochemistry for neutrophil elastase in each group of mice. Scale bars, 50 μ m. **h** The number of neutrophil elastase positive cells were counted and compared. **i**, **j** Relative mRNA expression levels of neutrophil-recruiting chemokines (*CXCL1* and *CXCL2*) from each group of mice were compared. **k**, **l** qRT-PCR for *CDH1* and *ACTA2* in each group of mice. $n = 3$ for control mice, $n = 5$ for NP mice, $n = 5$ for NP mice treated with inhibitor mixture, $n = 5$ for NP mice treated with dexamethasone (**c–e** and **h–l**), $n = 6$ for control mice, $n = 10$ for NP mice, $n = 10$ for NP mice treated with inhibitor mixture, $n = 10$ for NP mice treated with dexamethasone (**f**). Statistical significance (**c–l**) was determined by Kruskal–Wallis tests ($P < 0.01$), followed by Mann–Whitney *U*-test for pairwise comparisons. * $P < 0.05$; ** $P < 0.01$. Data are shown as means \pm s.e.m.

markers such as EDA-fibronectin, vimentin, α -SMA, and collagen-1.⁴⁰ Generally, SMAD3 forms a complex with SMAD4, and the activated SMAD3/SMAD4 complex is translocated to the nucleus where it modulates the transcription of target genes.⁴¹ However, IFN- γ treatment did not induce the activation of SMAD2 and SMAD3 (Fig. 3f). Furthermore, knockdown of SMAD3 did not result in morphological changes or restoration of the levels of EMT markers (Figure S5A–C). As reported previously, the expression of TGF- β 1 is decreased in both CRSsNP and CRSwNP patients.⁴² Therefore, it seems that IFN- γ induces the EMT independently of HIF-1 α and SMAD activation.

We next explored the effect of IFN- γ on epithelial barrier function under ALI conditions in vitro. The IFN- γ -induced EMT increased the migration capacity and decreased the TEER of cells (Figs. 2 and 5). However, pretreatment with the inhibitor mixture prevented the reduction in the TEER (Fig. 5e). Previously, Steelant et al. reported that IFN- γ had no effect on the epithelial permeability of isolated hNECs.⁴³ However, Ahdieh et al. showed that IFN- γ accelerated the healing of wounds in lung epithelium.⁴⁴ In addition, Soyka et al. reported that IFN- γ stimulation of

epithelial cells cultured under ALI conditions decreased the TEER and the levels of tight junction proteins.¹⁹ We speculate that differences in the materials and methodologies used, such as cell type and ALI culture environment, may explain these discrepant results.

Although the anatomy of the sinuses of mice is not identical to that of humans, mice possess the same respiratory epithelium and sinus cavities.⁴⁵ The mouse model of NPs used in this study³¹ exhibits allergic inflammation with eosinophilic infiltration and a Th2-biased inflammatory response. However, the NP model showed not only Th2 but also Th1 and Th17 responses,³¹ as is frequently observed in Asian patients with CRS with or without NPs.^{5,6,8} Indeed, the mouse model showed several neutrophilic features, including marked neutrophil infiltration and high-level IFN- γ expression (Fig. 6e–h). Administration of OVA and SEB resulted in upregulation of the mRNA and protein levels of IFN- γ (Fig. 6e, f). These neutrophilic features were reversed by application of p38 and ERK inhibitors, but not dexamethasone. Recent studies have used this model to evaluate epithelial remodeling, the therapeutic benefit of anti-polyp treatment, and

various host immunological characteristics.^{16,46,47} Thus, we considered this mouse model of NPs to be suitable for evaluating the role of IFN- γ in CRS.

In conclusion, our findings identified an important mechanism of neutrophil-dominant CRS. Our data suggest that controlling the IFN- γ -induced EMT pathways (for example, using inhibitors of p38 and ERK pathways) has therapeutic potential for neutrophil-dominant inflammation.

MATERIALS AND METHODS

Human subjects

Patients were enrolled in this study after providing written informed consent under protocols approved by the Internal Review Board of Seoul National University Hospital (SNUH) Boramae Medical Center (No. 06-2012-109) and SNUH (C-1708-054-876). The demographic characteristics of the patients are summarized in Table 1 (see the Online Supplementary Methods).

Culture and cytokine stimulation of epithelial cell lines

RPMI 2650 cells derived from the nasal septum were used in this study (Korean Cell Line Bank, Seoul, South Korea). Normal hNECs (PromoCell, Heidelberg, Germany) were cultured in airway epithelial cell growth medium (PromoCell) (see the Online Supplementary Methods).

ALI culture system

Passage 1 or 2 normal hNECs and polyp-derived nasal epithelial cells were seeded on 0.4 μ m, 0.33 cm² polyester Transwell inserts (Costar, Corning, NY, USA) at a density of 1×10^5 per well. Cells were cultured in a 1:1 mixture of BEGM [Lonza, Basel, Switzerland]: Dulbecco's modified Eagles' medium (DMEM) containing the same concentrations of all supplements, as described in the Supplementary Methods. The cells were cultured submerged for the first

9 days. The culture medium was changed on day 1 and refreshed every other day thereafter. After 9 days, an ALI was created by removing the medium from the apical compartment and feeding the cultures from the basal compartment only for 21 days (see the Online Supplementary Methods).

Immunofluorescence and confocal microscopy

Cells were cultured on cover slips and exposed to IL-5, TNF- α , IFN- γ , IL-17A, IL-6, IL-8, eotaxin1, or eotaxin2 (100 ng/ml) for 48 h (see the Online Supplementary Methods).

Immunoblotting

Proteins were separated in 8–15% sodium dodecyl sulfate-polyacrylamide gels, and transferred to Immobilon-P (Millipore, Billerica, MA, USA). Membranes were incubated sequentially with indicated primary and secondary antibodies; the antibodies used are specified in Table S1 (see the Online Supplementary Methods).

Transfection of siRNAs

Cells at 60% confluence were transfected with siRNAs using RNAi-MAX reagent (Invitrogen, Carlsbad, CA, USA). The phosphodiester RNA oligonucleotides for SMAD3, HIF-1 α , STAT1, and ICSBP were synthesized by IDT (Coralville, IO, USA). The siRNA sequences are shown in Table S2. Stealth RNAi negative control duplex (Invitrogen) was utilized as a control (see the Online Supplementary Methods).

Transient transfection and luciferase activity assay

For transient transfections, RPMI 2650 cells were seeded at approximately 5×10^5 per well in a six-well plate at 24 h before transfection. Plasmids were transfected into cells using Lipofectamine 3000 reagent (Invitrogen). Briefly, the reporter plasmid (1 μ g) and pCMV- β -gal vector (1 μ g) were diluted with Opti-MEM and mixed with diluted Lipofectamine 3000 reagent. After incubation for 20 min at room temperature, these mixtures were added to each well. At 8 h post transfection, the medium was replaced with RPMI 1640 medium containing 10% fetal bovine serum and antibiotics. Cells were allowed to recover for 24 h and subsequently stimulated as indicated. Cell lysates were prepared and subjected to luciferase assay using the Luciferase Assay System (Promega, Madison, WI, USA) according to the manufacturer's instructions. β -galactosidase activity was used as the internal control.

Fractionation of cytoplasmic and nuclear components

Cells stimulated or not with IFN- γ (Peprotech, Rocky Hill, CT, USA) were centrifuged at $800 \times g$ for 5 min and gently homogenized in a hypotonic solution containing 20 mM Tris/HCl (pH 7.8), 1.5 mM MgCl₂, 10 mM KCl, 0.2 mM EDTA, 0.5% NP-40, 0.5 mM dithiothreitol, and 0.5 mM phenylmethylsulfonyl fluoride. The cell lysates were centrifuged at $3000 \times g$ for 10 min at 4°C, and the supernatant was collected as the cytosolic fraction (see the Online Supplementary Methods).

MTT cell viability assay

The cytotoxicity of IFN- γ (Peprotech), SB203580, and PD98059 (Cell Signaling, Danvers, MA, USA) against hNECs was evaluated by MTT (Sigma-Aldrich, St. Louis, MO, USA) viability assay (see the Online Supplementary Methods).

TEER measurement

Epithelial integrity was evaluated by measuring the TEER using an EVOM/Endohm chamber (WPI, Sarasota, FL, USA). Cells treated with medium alone served as the control. For ALI inserts, 0.2 and 0.5 ml of pre-equilibrated medium were added to the apical and basolateral reservoirs, respectively. ALI-cultured cells were incubated with vehicle or inhibitor mixture for 1 h, and recombinant human IFN- γ (Peprotech) was added to the basolateral reservoirs.

Table 1. Patient characteristics and methodologies used

| Total no. of subjects | Control N = 20 | CRSsNP | | CRSwNP | |
|---|-------------------|---------------|---------------|---------------|-----------------|
| | | N = 22 | N = 42 | N = 39 | N = 35 |
| Tissue used | UP | UP | UP | NE-NP | E-NP |
| Age (yr), mean (SD) | 49 (18) | 53 (20) | 51 (14) | 50.00 (15) | 52.02 (14.15) |
| Atopy, N | 4 | 8 | 15 | 16 | 18 |
| Asthma, N | 0 | 1 | 1 | 0 | 1 |
| Aspirin intolerance | 0 | 0 | 0 | 0 | 0 |
| Nasal steroid | 1 | 0 | 0 | 0 | 0 |
| Inhaled steroid | 0 | 0 | 0 | 0 | 0 |
| Oral steroid | 0 | 0 | 0 | 0 | 0 |
| Lund-Mackay CT score | 0.6(2.0) | 7.9 (2.6) | 14.9 (5.9) | 15.2 (5.7) | 13.67 (5.19) |
| Blood eosinophil number (/mm ³) | 93.9 (57.6) | 138.2 (102.1) | 130.3 (102.7) | 146.4 (114.1) | 135.70 (104.05) |
| <i>Methodologies used</i> | | | | | |
| Tissue IHC | N = 7 | N = 11 | N = 9 | N = 10 | N = 8 |
| Tissue IF | N = 7 | N = 11 | N = 9 | N = 10 | N = 8 |
| Homogenate | N = 6 | N = 11 | N = 33 | N = 22 | N = 27 |
| ALI epithelial culture | N = 7 | N = 0 | N = 0 | N = 7 | N = 0 |

CRSwNP chronic rhinosinusitis with nasal polyp, CRSsNP chronic rhinosinusitis without nasal polyp, UP uncinat process, NE non-eosinophilic, E-eosinophilic, NP nasal polyp, CT computed tomography, IHC immunohistochemistry, IF immunofluorescence



After cytokine treatment, TEER was measured in triplicate for each group from 0 to 72 h.

Boyden chamber migration assay

For cell migration, cells were seeded at 2.0×10^4 /200 μ l per well in the upper chamber of 24-transwell plates (Costar). The empty upper chamber was filled with hNECs, which were diluted in airway epithelial cell growth medium without serum. The lower chamber was filled with airway epithelial cell growth medium containing 5% serum growth supplement mixture. After incubation for 1 h at 37 °C with vehicle (DMSO + PBS) or SB203580 and PD98059 mixture, IFN- γ recombinant peptide was added to the upper chamber (see the Online Supplementary Methods).

Wound-healing migration assay

A monolayer wound-healing assay was performed to analyze cell migration in vitro. A total of 2.5×10^5 hNECs was collected and plated in a 24-well plate. At 100% confluence, sterile tips were used to scratch cell layers, which were subsequently washed with PBS, and cultured with airway epithelial cell growth medium (PromoCell) containing supplements and the presence or absence of IFN- γ (100 ng/ml). Cells were photographed (phase contrast microscope) at 0 and 48 h after scratching. The area filled by migrated cells was measured between the two boundaries of the cellular area using ImageJ software (NIH Image processing analysis, <http://rsb.info.nih.gov/ij/>). The amount of healing on each of the scratch wounds was calculated as follows: wound healing rate (%) = $(A_0 - A_t)/A_0 \times 100\%$, where A_0 and A_t represent the initial wound area and the wound area at time t , respectively. Each assay was performed in three independent experiments.

Quantitative real-time PCR for EMT markers, inflammatory markers, and chemokines

Total RNA was extracted using QIAshredder columns and the RNeasy Mini RNA isolation kit (Qiagen, Valencia, CA, USA). Sequentially, cDNA was synthesized using a cDNA QuantiTect reverse transcription kit (Qiagen). The mRNA levels were evaluated using semi-quantitative real-time PCR (qRT-PCR) analysis as described previously²⁴ (see the Online Supplementary Methods).

Murine nasal polyp model and tissue preparation

Thirty-six BALB/C mice (4 weeks old, 20–25 g) were purchased (Central Laboratory Animals, Seoul, South Korea) and kept in specific pathogen-free rooms. All animal experiments were approved by the IACUC of Seoul National University (No. SNU-150311-1-1) and complied with governmental and international guidelines on animal experimentation. A murine NP model was generated from a mouse allergic rhinosinusitis model with minor amendments, as described previously¹⁶ (see the Online Supplementary Methods).

Immunohistochemistry

IFN- γ , E-cad, conventional MAPK signaling molecules (p-ERK and p-p38), EMBP, and neutrophil elastase were immunostained in paraffin sections (4 μ m) of sinonasal tissues. Sinonasal tissues were fixed in 4% paraformaldehyde at 4 °C for 24 h, then dehydrated in ethanol and sequential concentrations of xylene before embedding them in paraffin. Paraffin sections (4 μ m) of sinonasal tissues were mounted on slide glasses and dried at room temperature for 24 h (see the Online Supplementary Methods).

Cytokines from nasal lavage fluid

Nasal lavage was collected as described previously.⁴⁸ After partial tracheal resection under deep anesthesia, a micropipette was inserted into the posterior choana through the tracheal opening in the direction of the upper airway. Each nasal cavity was perfused gently with 200 μ l of PBS, and fluid from the nostril was collected and centrifuged. Supernatants were stored at –80 °C.

The amounts of IFN- γ in the nasal fluids from mice were quantified using the Legend Max ELISA kit (BioLegend, San Diego, CA, USA). The lower detection limit of all of these ELISA kits was 15.6 pg/ml. Each assay was performed in triplicate.

Human tissue extracts

Freshly obtained tissue specimens were weighed, and tissue with a volume of 110 μ l was used for analysis. PBS (1 ml) supplemented with 0.05% Tween 20 (Sigma-Aldrich) and 1% protease inhibitor cocktail (Sigma-Aldrich) was added to the tissue, and each sample was homogenized using a Bullet Blender Blue (Next Advance, Averill Park, NY, USA) at setting 7 for 8 min at 48 °C (see the Online Supplementary Methods).

Statistical analysis

Statistical analyses were performed using SPSS 23.0 software (SPSS, Chicago, IL, USA). Differences in normally distributed data were evaluated by Student's t -test and those in non-normally distributed data by the equivalent non-parametric test (Mann–Whitney U -test, Kruskal–Wallis test, or Wilcoxon signed-rank test). Associations between the IF signal intensities of IFN- γ and E-cad, and between the IFN- γ IHC signal intensity and the E-cad expression score were analyzed by calculating Spearman's correlation coefficient. All statistical tests were two-sided, and statistical significance is indicated as $*P < 0.05$ and $**P < 0.01$. Data are the means \pm standard errors of the mean of at least three independent experiments. Illustrative figures were generated using Prism version 8.0 (GraphPad Software Inc., La Jolla, CA, USA) and SigmaPlot version 10.0 (Systat Software Inc., San Jose, CA, USA).

ACKNOWLEDGEMENTS

This research was supported by a grant of the Korea Health Technology R&D Project through the Korea Health Industry Development Institute (KHIDI), funded by the Ministry of Health & Welfare, Republic of Korea (grant number: HI17C1669).

AUTHOR CONTRIBUTIONS

Conception and design: M.G.L., H.-W.S.; acquisition of data: M.G.L., D.W.K., R.K., S.H.S.; analysis and interpretation of data: M.G.L., D.W.K., Y.-M.K., D.H.H., H.-J.K., D.-Y.K., C.-S.R., J.-W.P., H.-W.S.; drafting the article or revising it critically for important intellectual content: M.G.L., J.-W.P., H.-W.S.

ADDITIONAL INFORMATION

The online version of this article (<https://doi.org/10.1038/s41385-019-0149-1>) contains supplementary material, which is available to authorized users.

Competing interests: The authors declare no competing interests.

Publisher's note: Springer Nature remains neutral with regard to jurisdictional claims in published maps and institutional affiliations.

REFERENCES

1. Hamilos, D. L. Chronic rhinosinusitis: epidemiology and medical management. *J. Allergy Clin. Immunol.* **128**, 693–707 (2011). quiz 708–699.
2. Wynn, R. & Har-El, G. Recurrence rates after endoscopic sinus surgery for massive sinus polyposis. *Laryngoscope* **114**, 811–813 (2004).
3. Payne, S. C. et al. Evidence for distinct histologic profile of nasal polyps with and without eosinophilia. *Laryngoscope* **121**, 2262–2267 (2011).
4. Bachert, C., Wagenmann, M., Hauser, U. & Rudack, C. IL-5 synthesis is upregulated in human nasal polyp tissue. *J. Allergy Clin. Immunol.* **99**(6 Pt 1), 837–842 (1997).
5. Van Bruaene, N. et al. T-cell regulation in chronic paranasal sinus disease. *J. Allergy Clin. Immunol.* **121**, 1435–1441 (2008). 1441 e1431–1433.
6. Van Zele, T. et al. Differentiation of chronic sinus diseases by measurement of inflammatory mediators. *Allergy* **61**, 1280–1289 (2006).
7. Mahdavinia, M. et al. Increased noneosinophilic nasal polyps in chronic rhinosinusitis in US second-generation Asians suggest genetic regulation of eosinophilia. *J. Allergy Clin. Immunol.* **135**, 576–579 (2015).

8. Zhang, N. et al. Different types of T-effector cells orchestrate mucosal inflammation in chronic sinus disease. *J. Allergy Clin. Immunol.* **122**, 961–968 (2008).
9. Cao, P. P. et al. Distinct immunopathologic characteristics of various types of chronic rhinosinusitis in adult Chinese. *J. Allergy Clin. Immunol.* **124**, 478–484.e1–2 (2009).
10. Wang, X. et al. Diversity of TH cytokine profiles in patients with chronic rhinosinusitis: a multicenter study in Europe, Asia, and Oceania. *J. Allergy Clin. Immunol.* **138**, 1344–1353 (2016).
11. Tomassen, P. et al. Inflammatory endotypes of chronic rhinosinusitis based on cluster analysis of biomarkers. *J. Allergy Clin. Immunol.* **137**, 1449–1456.e1444 (2016).
12. Small, C. B., Stryzszak, P., Danzig, M. & Damiano, A. Onset of symptomatic effect of mometasone furoate nasal spray in the treatment of nasal polyposis. *J. Allergy Clin. Immunol.* **121**, 928–932 (2008).
13. Wen, W. P. et al. Increased neutrophilia in nasal polyps reduces the response to oral corticosteroid therapy. *J. Allergy Clin. Immunol.* **129**, 1522 (2012).
14. Hew, M. et al. Relative corticosteroid insensitivity of peripheral blood mononuclear cells in severe asthma. *Am. J. Respir. Crit. Care Med.* **174**, 134–141 (2006).
15. Hupin, C. et al. Features of mesenchymal transition in the airway epithelium from chronic rhinosinusitis. *Allergy* **69**, 1540–1549 (2014).
16. Lee, M. et al. Sirtuin 1 attenuates nasal polypogenesis by suppressing epithelial-to-mesenchymal transition. *J. Allergy Clin. Immunol.* **137**, 87–98.e87 (2016).
17. Acloque, H., Adams, M. S., Fishwick, K., Bronner-Fraser, M. & Nieto, M. A. Epithelial-mesenchymal transitions: the importance of changing cell state in development and disease. *J. Clin. Invest.* **119**, 1438–1449 (2009).
18. Liu, X. Inflammatory cytokines augments TGF- β 1-induced epithelial-mesenchymal transition in A549 cells by up-regulating T β 1. *Cell Motil. Cytoskeleton* **65**, 935–944 (2008).
19. Soyka, M. B. et al. Defective epithelial barrier in chronic rhinosinusitis: the regulation of tight junctions by IFN- γ and IL-4. *J. Allergy Clin. Immunol.* **130**, 1087–1096.e1010 (2012).
20. Bruewer, M. et al. Interferon- γ induces internalization of epithelial tight junction proteins via a macropinocytosis-like process. *FASEB J.* **19**, 923–933 (2005).
21. Sung, J. Y. et al. Interferon consensus sequence-binding protein (ICSBP) promotes epithelial-to-mesenchymal transition (EMT)-like phenomena, cell motility, and invasion via TGF- β signaling in U2OS cells. *Cell Death Dis.* **5**, e1224 (2014).
22. Lee, M., Khalmuratova, R., Kim, D. W. & Shin, H. W. IFN- γ contributes to nasal polypogenesis by inducing epithelial-to-mesenchymal transition via non-smad pathway [abstract]. In *World Allergy Congress* (Seoul, Korea, 2015).
23. Wang, E. T., Zheng, Y., Liu, P. F. & Guo, L. J. Eosinophilic chronic rhinosinusitis in East Asians. *World J. Clin. Cases* **2**, 873–882 (2014).
24. Shin, H. W. et al. Hypoxia-inducible factor 1 mediates nasal polypogenesis by inducing epithelial-to-mesenchymal transition. *Am. J. Respir. Crit. Care Med.* **185**, 944–954 (2012).
25. Yeh, T. H. et al. Increased communication among nasal epithelial cells in air-liquid interface culture. *Laryngoscope* **117**, 1439–1444 (2007).
26. Muller, L., Brighton, L. E., Carson, J. L., Fischer, W. A., 2nd & Jaspers, I. Culturing of human nasal epithelial cells at the air liquid interface. *J. Vis. Exp.* (2013).
27. Gough, D. J., Levy, D. E., Johnstone, R. W. & Clarke, C. J. IFN- γ signaling—does it mean JAK-STAT? *Cytokine Growth Factor Rev.* **19**, 383–394 (2008).
28. Platanias, L. C. Mechanisms of type-I- and type-II-interferon-mediated signalling. *Nat. Rev. Immunol.* **5**, 375–386 (2005).
29. Ramana, C. V., Gil, M. P., Schreiber, R. D. & Stark, G. R. Stat1-dependent and -independent pathways in IFN- γ -dependent signaling. *Trends Immunol.* **23**, 96–101 (2002).
30. Sung, J. Y., Kim, H., Kim, Y. N., Na, Y. S. & Park, B. K. Interferon consensus sequence binding protein-induced cell proliferation is mediated by TGF- β signaling and p38 MAPK activation. *Lab. Invest.* **91**, 1304–1313 (2011).
31. Kim, D. W. et al. Staphylococcus aureus enterotoxin B contributes to induction of nasal polypoid lesions in an allergic rhinosinusitis murine model. *Am. J. Rhinol. Allergy* **25**, e255–e261 (2011).
32. Sun, C., Ouyang, H. & Luo, R. Distinct characteristics of nasal polyps with and without eosinophilia. *Braz. J. Otorhinolaryngol.* **83**, 66–72 (2017).
33. Baba, S. et al. T-cell phenotypes in chronic rhinosinusitis with nasal polyps in Japanese patients. *Allergy Asthma Clin. Immunol.* **11**, 33 (2015).
34. Van Bruaene, N. et al. Inflammation and remodelling patterns in early stage chronic rhinosinusitis. *Clin. Exp. Allergy* **42**, 883–890 (2012).
35. Schleimer, R. P. Immunopathogenesis of chronic rhinosinusitis and nasal polyposis. *Annu. Rev. Pathol.* **12**, 331–357 (2017).
36. Stockinger, A., Eger, A., Wolf, J., Beug, H. & Foisner, R. E-cadherin regulates cell growth by modulating proliferation-dependent beta-catenin transcriptional activity. *J. Cell Biol.* **154**, 1185–1196 (2001).
37. Kim, N. G., Koh, E., Chen, X. & Gumbiner, B. M. E-cadherin mediates contact inhibition of proliferation through Hippo signaling-pathway components. *Proc. Natl Acad. Sci. USA* **108**, 11930–11935 (2011).
38. Raundhal, M. et al. High IFN- γ and low SLPI mark severe asthma in mice and humans. *J. Clin. Invest.* **125**, 3037–3050 (2015).
39. Jarjour, N. N. et al. Severe asthma: lessons learned from the National Heart, Lung, and Blood Institute Severe Asthma Research Program. *Am. J. Respir. Crit. Care Med.* **185**, 356–362 (2012).
40. Hackett, T. L. et al. Induction of epithelial-mesenchymal transition in primary airway epithelial cells from patients with asthma by transforming growth factor- β 1. *Am. J. Respir. Crit. Care Med.* **180**, 122–133 (2009).
41. Derynck, R. & Zhang, Y. E. Smad-dependent and Smad-independent pathways in TGF- β family signalling. *Nature* **425**, 577–584 (2003).
42. Van Bruaene, N. et al. TGF- β signaling and collagen deposition in chronic rhinosinusitis. *J. Allergy Clin. Immunol.* **124**, 253–259.e1–2 (2009).
43. Steelant, B. et al. Impaired barrier function in patients with house dust mite-induced allergic rhinitis is accompanied by decreased occludin and zonula occludens-1 expression. *J. Allergy Clin. Immunol.* **137**, 1043–1053.e1045 (2016).
44. Ahdieh, M., Vandenbos, T. & Youakim, A. Lung epithelial barrier function and wound healing are decreased by IL-4 and IL-13 and enhanced by IFN- γ . *Am. J. Physiol. Cell. Physiol.* **281**, C2029–C2038 (2001).
45. Jacob, A. & Chole, R. A. Survey anatomy of the paranasal sinuses in the normal mouse. *Laryngoscope* **116**, 558–563 (2006).
46. Kim, S. W. et al. Resveratrol prevents development of eosinophilic rhinosinusitis with nasal polyps in a mouse model. *Allergy* **68**, 862–869 (2013).
47. Lee, K. I. et al. Cigarette smoke promotes eosinophilic inflammation, airway remodeling, and nasal polyps in a murine polyp model. *Am. J. Rhinol. Allergy* **28**, 208–214 (2014).
48. Rhee, C. S. et al. Allergen-independent immunostimulatory sequence oligodeoxynucleotide therapy attenuates experimental allergic rhinitis. *Immunology* **113**, 106–113 (2004).



Open Access This article is licensed under a Creative Commons Attribution 4.0 International License, which permits use, sharing, adaptation, distribution and reproduction in any medium or format, as long as you give appropriate credit to the original author(s) and the source, provide a link to the Creative Commons license, and indicate if changes were made. The images or other third party material in this article are included in the article's Creative Commons license, unless indicated otherwise in a credit line to the material. If material is not included in the article's Creative Commons license and your intended use is not permitted by statutory regulation or exceeds the permitted use, you will need to obtain permission directly from the copyright holder. To view a copy of this license, visit <http://creativecommons.org/licenses/by/4.0/>.

© The Author(s) 2019

